

Figure S1 Independent effects on the genotype-phenotype (G-P) map of bioenergetic parameters ΔG_1 , E_{diff} and N_{TF} . Horizontal axis: the number of mismatched bits between the binding site and the transcription factor's binding motif. Vertical axis: the phenotype, which in this case is the expression level normalized to a scale of zero to one. ΔG_1 and E_{diff} are in units of $k_b T$. (A) effect of ΔG_1 , the unit of change in the free energy of formation contributed by a single bit for binding between transcription factor and target binding site, in steps of $0.0825 k_b T$. (B) effect of E_{diff} , the free energy of formation for general nonspecific binding relative to specific binding, in steps of $1 k_b T$. (C) effect of exponential increase in N_{TF} , the number of transcription factor molecules, stepping the exponent 1.25 units and rounding to the nearest integer. N_{TF} on the exponential scale has the same effect on the G-P map as does E_{diff} on the linear scale, and values for N_{TF} can be chosen for panel C's condition of $E_{diff} = 0$ that match, to the nearest integer, the curves of panel B. To avoid redundancy, we therefore varied only E_{diff} in the analyses.

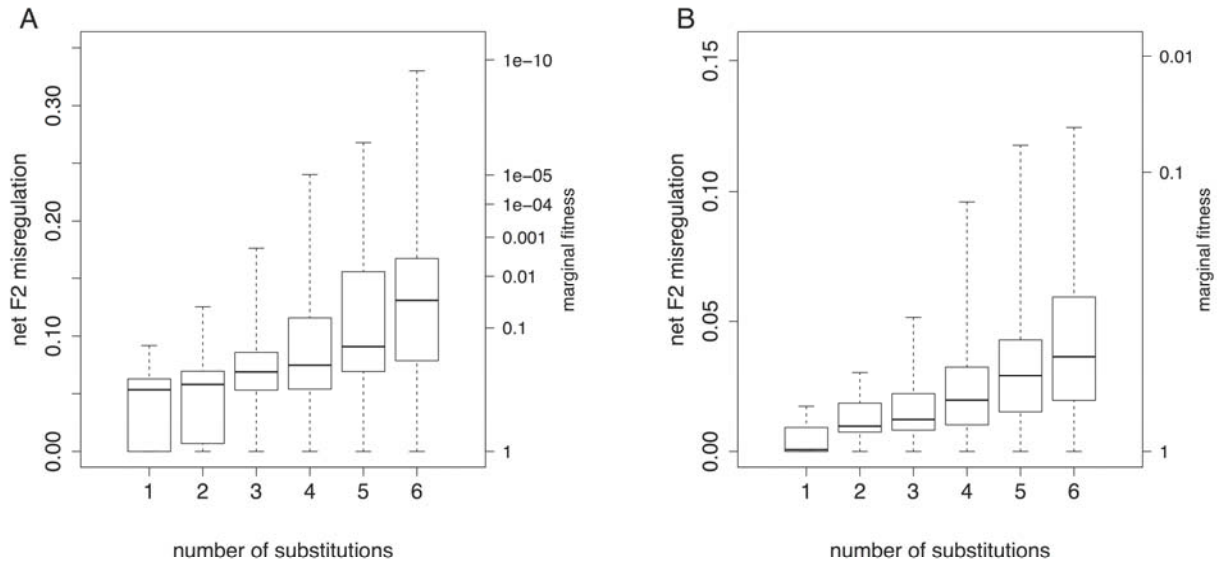


Figure S2 Effect of genotypic divergence on median net F2 hybrid misregulation and corresponding fitness under directional selection. Genotypic divergence is represented by the number of substitutions required to evolve between the optimal phenotypes at the beginning and end of the selection period. Bioenergetic parameters specifying the G-P map were held constant and only the initial optimal phenotype was varied. (A) Evolving towards intermediate phenotype (final $P_{opt} = 0.5$). (B) Evolving towards extreme phenotype (final $P_{opt} = 1.0$). Hybrid fitness follows equation 4. Note the different scales. Box plots show median, quartiles and full ranges.

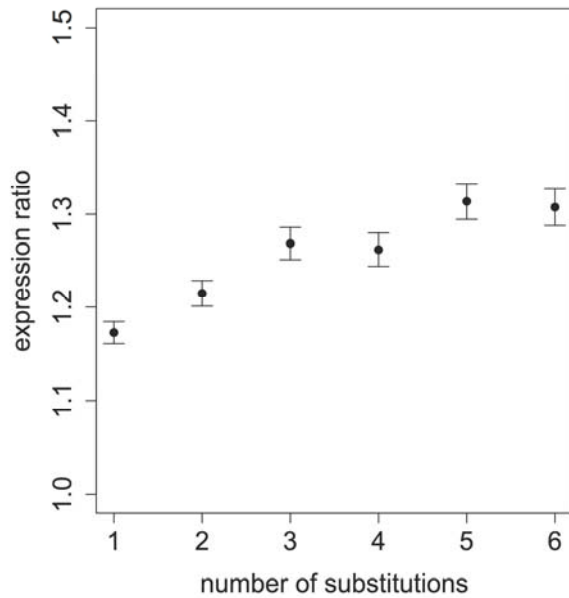


Figure S3 Effect of genotypic divergence on asymmetric expression between parental orthologs in F1 hybrids. Genotypic divergence is represented by the number of substitutions required to evolve between the optimal phenotypes at the beginning and end of the selection period, with selection for reduced expression towards an intermediate final phenotype of $P_{opt} = 0.5$. Bioenergetic parameters specifying the genotype-phenotype map were held constant and only the initial optimal phenotype was varied. Asymmetry is shown as the mean (s.e.) expression ratio.

File S1

Supplemental materials

Derivation of the competitive inhibition term in fractional occupancy

Fractional occupancy of a TF on its binding site is reduced in the presence of a competitive inhibitor, and in a heterozygote, TF molecules coded by different TF alleles compete with one another. Here we derive equation (3), expressing the Michaelis-Menten model for competitive binding in terms of the statistical physics model of Gerland et al. (2002). From Michaelis and Menten (1913), equilibrium fractional occupancy in the absence of a competitor is

$$\frac{[B_{TF}]}{[B]} = \frac{[TF]}{[TF] + \frac{k_u}{k_b}}$$

where [] denotes concentration, B represents binding sites (whether occupied or unoccupied), TF is the unbound transcription factor of interest, B_{TF} is the bound TF-binding site complex, k_u is the rate that a bound TF dissociates from its binding site, and k_b is the rate that a free TF binds. In the notation in this paper, fractional occupancy of the TF of interest on its binding site is $\theta = [B_{TF}]/[B]$. Given an arbitrary unit of volume, which we consider to be the intracellular environment, concentrations can be expressed as numbers, such that $[TF]$ becomes N_{TF} , the number of molecules of the TF of interest. Substituting for θ and canceling terms,

$$k_u/k_b = e^{-m\Delta G_i - E_{aiv}}.$$

From Michaelis and Menten (1913), equilibrium fractional occupancy in the presence of a competitor is expressed as

$$\frac{[B_{TF}]}{[B]} = \frac{[TF]}{[TF] + \left(1 + [C] \frac{k_{bc}}{k_{uc}}\right) \frac{k_u}{k_b}}$$

where $[C]$ is the concentration of the competitive inhibitor (here, the TF coded by the alternative allele), k_{uc} is the rate that the bound competitor dissociates from the binding site and k_{bc} is the rate that a free competitor binds; by symmetry, $k_{uc}/k_{bc} = e^{-m\Delta G_i - E_{diff,c}}$. Given an arbitrary unit of volume, $[C]$ becomes N_{TFc} , the number of molecules of the competing TF. In our notation, fractional occupancy of a specified TF in the presence of the TF of the competing allele is $\theta' = [B_{TF}]/[B]$. By assuming $E_{diff,c} = E_{diff}$, $N_{TFc} = N_{TF}$, and substituting,

$$\theta' = \frac{N_{TF}}{N_{TF} + \alpha e^{-m\Delta G_i - E_{diff}}}$$

where $\alpha = 1 + N_{TF} e^{m\Delta G_i + E_{diff}}$.

Effects of evolutionary distance and the direction of selection

We define evolutionary distance as the number of substitutions required to go from the initial to the final phenotype. Here we show an interaction between the direction of selection and evolutionary distance. Selection from intermediate ($P_{opt} = 0.5$) towards more extreme phenotypic expression ($P_{opt} = 1.0$, and by the symmetry of the relationship between the proportion of matched and mismatched bits and expression, $P_{opt} = 0.0$) provides a strong evolutionary constraint on the evolution of hybrid incompatibility relative to selection toward intermediate expression levels, and the degree of constraint is sensitive to evolutionary distance.

Methods: To assess the role of the direction of selection, we evolved populations from an intermediate phenotype of $P_{opt} = 0.5$ to an extreme phenotype of $P_{opt} = 1.0$, as in the simulations in the body of the paper. We compared these results to selection in the opposite direction, from extreme phenotype of $P_{opt} = 1.0$ to the intermediate phenotype of $P_{opt} = 0.5$. To assess the role of evolutionary distance on the evolution of hybrid incompatibility, we evolved populations to the same final phenotype from different initial phenotypes, rather than varying the bioenergetic parameters, which would change the shapes of the G-P map and fitness landscape. Thus, evolution proceeded for varying distances along the same genotypic landscape toward an end point of phenotype $P_{opt} = 0.5$ (if selection was for expression from the extreme towards an intermediate phenotype) or $P_{opt} = 1.0$ (if selection was for expression from an extreme towards an extreme phenotype).

Results: The effect on hybrid incompatibility of the number of substitutions required to reach the final phenotype can be seen in Figure S2. When selection was toward intermediate expression (Figure S2A), increasing the required number of substitutions increased the average number of spurious TF-binding site matches in the hybrid. However, selection toward more extreme expression had a constraining effect on the evolution of HI, three to five times lower depending on the number of substitutions required to reach the end phenotype.

When selection was for increased expression (Figure S2B), increasing the required number of substitutions increased the average number of mismatches, thus median HI, that arose in F2 hybrids when the parents had zero mismatches. HI was minimal in the F1 generation because mismatched allelic combinations were recessive under the parameter combinations we used. For a given level of divergence, median HI was higher under selection towards an intermediate phenotype compared to selection towards an extreme phenotype due to the relative slopes of

our G-P map and fitness landscape at the derived parental phenotypes (see Figure 2; and effect of slope, in the Results in the main text).

Regulatory divergence and asymmetric expression of orthologs in F1 hybrids

The degree of hybrid incompatibility depends on the extent that the hybrid phenotype is misregulated relative to the genotype that results in the optimal phenotype. Since phenotype depends on gene expression, we can expect that the extent of misregulation may depend not only on the number of inappropriate mismatches that have evolved between parental populations, but where along the G-P map and fitness landscape those mismatches lie. Here we test these predictions by separating the effects of the location along the G-P map where adaptation occurs, and the number of new mismatches that the parental populations must accumulate to reach that position. Our proxy for the effect of location along the G-P map is the direction of selection towards the final optimal phenotype. Toward $P_{opt} = 1.0$, interpopulation mismatches accumulate along a locally more shallowly sloping region of a given G-P map (Figure 2, main text) whereas toward $P_{opt} = 0.5$, interpopulation mismatches accumulate along a locally steeper region. Our metric is the relative gene expression, in F1 hybrids, of parental orthologs of the *cis*-regulated locus. We show that the degree of asymmetrical expression of parental orthologs depends on both the direction of selection and evolutionary distance.

Methods: For each F1 individual, we calculated the expression level of each parental ortholog of the *cis*-regulated locus. Using those, we calculated the ratio as the expression of the more highly expressed allele divided by that of the less expressed allele. Expression is symmetrical when the expression ratio is 1.0 and asymmetrical otherwise. To avoid potential confounding effects of differing fitness landscapes, we evolved parental populations on the same fitness landscape but from different starting points to reach the final optimum. We compared

evolution from extreme optimal phenotypes of $P_{opt} = 1.0$ toward intermediate optima of $P_{opt} = 0.5$ to evolution in the opposite direction, from intermediate ($P_{opt} = 0.5$) to extreme ($P_{opt} = 1.0$) expression. When asymmetry exists, we expect its degree to depend on genetic distance from the ancestral to derived expression levels in the diploid parents — the number of substitutions required for the parental populations to evolve from the initial optimum to the final optimum — with less asymmetry when fewer changes are required.

Results: Parental orthologs of the *cis*-regulated locus showed asymmetric expression in F1 hybrids only under directional selection towards intermediate expression. The magnitude of asymmetry was a function of the divergence between ancestral and derived populations (Figure S3), increasing from a mean of 1.17 to 1.3 with the number of substitutions required to reach the final phenotype of 0.5. Asymmetric expression was observed in individual replicates regardless of the extent of HI. Within parental populations, asymmetry between derived alleles was negligible (mean parental expression ratio = 1.0006 ± 0.0001). This is consistent with our predictions. Under directional selection towards high expression, asymmetry in F1 hybrids was low regardless of genetic divergence (mean expression ratio after six substitutions = 1.014 ± 0.001). In this case, a perfect fit was favored between the TF and its binding site, which reduced the opportunity for asymmetric expression because two unique perfect fits are equally mismatched to one another.